ISSN: 2319-5967
ISO 9001:2008 Certified
International Journal of Engineering Science and Innovative Technology (IJESIT)
Volume 2, Issue 1, January 2013

Modeling the Transport-Diffusion of a Passive Pollutant in the Bay Of Martil (Morocco)

EL OUAHDANI Driss[1], ECHARRI Raouf[2], STITOU Mostafa[3]
Laboratory of water, study and environmental analysis Faculty of Sciences, Tétouan Morocco

ABSTRACT The purpose of this study is to establish a mathematical model that describes the transport of a passive pollutant linked to discharge of sewage into the Bay of Martil Morocco. We are interested in this paper to a numerical simulation by finite volume scheme, adaptive and balanced, for a flow of real non-permanent, non-uniform and govern in areas of shallow water. We speak of free surface flows or flows in shallow water. These flows are governed by the system of equations "Saint Venant" consists of the continuity equation and the equation of dynamics. In this system of hydrodynamic equations we will couple the equation transport-diffusion to take into account the transport and diffusion of a non active pollutant in the flow. The mathematical approach is therefore, in its first part, to solve the system of "Saint-Venant", which is a system of partial differential and nonlinear hyperbolic equations. It is thus impossible to solve this system analytically in a general case. Consequently, a numerical solution of this system is needed. Simulate the free surface flow amounts to solving the system of "Saint Venant" using a robust numerical scheme, ie capable of giving a numerical solution closer to reality whatever the peculiarities of flow.

Key words: **Transport, Diffusion, Flow, Pollutant, Bay.**

I. INTRODUCTION

Forecasts of the risk posed to water quality in the Bay of Martil (Morocco) because of pollution from different sources mainly sources of wastewater discharges, can play a vital role in establishing a down model of a sea outfall of sewerage. The numerical model presented here solves the hydrodynamics in conjunction with the passive transport of species, allowing the user to estimate the transport and diffusion of pollutants, the concentration distribution, and the residence time of the basin. This document describes the transport and dispersion of effluents by the finite volume method with a solution of high definition with a non-homogeneous hyperbolic system of equations that represent shallow-water flow processes transport of pollutants. The computational mesh is an unstructured mesh, triangular, and dynamically adaptive. We use the Roe Riemann solver for advection flow, integration in time is performed using a Runge-Kutta.In recent years, and there has been increasing interest in the design of numerical schemes based on non-linear conservation laws. A particular challenge is to obtain high-order accurate solutions in space and time for flows over complicated bed topography. The non-linear shallow-water equations, utilizing upwind methods based on approximate Riemann solvers. Such solvers include Roe's method [10], monotonic upstream schemes for conservation laws (MUSCL) in curvilinear coordinate systems [11][12], essentially non-oscillatory schemes [13], the weighted essentially non-oscillatory method [13].The paper is organized as follows:

- The first part provides an overview of the work and methods used for solving the problem.
- The second part deals with the various governing equations in this application.
- The third part gives the numerical method used for the resolution of this system.
- The fourth part deals with the system of the mesh used.
- The fifth section presents the results of work.
- And the sixth section discusses these results by giving a general conclusion.

II. ESTABLISHMENT OF GOVERNING EQUATIONS

In conservation form, the two-dimensional non-linear shallow water equations are given by Equations (1) to (3) below [14]. The depth-averaged continuity equation is

$$\frac{\partial h}{\partial t} + \frac{\partial (hu)}{\partial x} + \frac{\partial (hv)}{\partial y} = 0 \qquad (1)$$

ISSN: 2319-5967
ISO 9001:2008 Certified
International Journal of Engineering Science and Innovative Technology (IJESIT)
Volume 2, Issue 1, January 2013

$$\frac{\partial(hu)}{\partial t}+\frac{\partial\left(hu^2+\frac{gh^2}{2}\right)}{\partial x}+\frac{\partial(huv)}{\partial y}=-gh\frac{\partial z_b}{\partial x}-\frac{S_{fx}}{\rho} \qquad (2)$$

$$\frac{\partial(hv)}{\partial t}+\frac{\partial\left(hv^2+\frac{gh^2}{2}\right)}{\partial x}+\frac{\partial(huv)}{\partial y}=-gh\frac{\partial z_b}{\partial y}-\frac{S_{fy}}{\rho} \qquad (3)$$

Where h is the total depth from the sea bed to the free surface, u and v are the depth-averaged velocity components in the Cartesian x and y directions, b_z is the bed elevation above a fixed horizontal datum, g the acceleration due to gravity, and et S_{fx} and S_{fy} are the bed shear stress components, defined as:

$$S_{fx}=\rho C_b u\sqrt{u^2+v^2}, \qquad S_{fy}=\rho C_b v\sqrt{u^2+v^2} \qquad (4)$$

Where ρ is the water density and C_b is the bed friction coefficient, which may be estimated from $C_b = gn_M^2/h^{1/3}$, where n_M is the Manning coefficient. Assuming the water pollutant mixture is fully mixed in the vertical direction, the depth-averaged pollution dispersion equation may be written in advection-diffusion form for a passive contaminant as:

$$\frac{\partial C}{\partial t}+u\frac{\partial C}{\partial x}+v\frac{\partial C}{\partial y}=\frac{\partial}{\partial x}\left(D_x\frac{\partial C}{\partial x}\right)+\frac{\partial}{\partial y}\left(D_y\frac{\partial C}{\partial y}\right) \qquad (5)$$

Where C is pollutant concentration, and Dx and Dy are pollutant diffusion coefficients in the x and y directions. Using matrix-vector notation, the coupled pollutant transport system can be written:

$$W_t+F_1(W)_x+F_2(W)_y-\tilde{F}_1(W)_x-\tilde{F}_2(W)_y=S(W) \qquad (6)$$

where W is the vector of dependent variables F_1, F_2 are the inviscid flux vectors, $\tilde{F}_1, \tilde{F}_2$ are diffusive flux vectors, S is the vector of source terms, and the subscripts x, y, and t denote partial differentiation. In full, the vectors are:

$$W=\begin{pmatrix}h\\hu\\hv\\hC\end{pmatrix}, F_1=\begin{pmatrix}hu\\hu^2+\frac{gh^2}{2}\\huv\\huC\end{pmatrix}, F_2=\begin{pmatrix}hv\\huv\\hv^2+\frac{gh^2}{2}\\hvC\end{pmatrix}, \tilde{F}_1=\begin{pmatrix}0\\0\\0\\\frac{\partial}{\partial x}\left(hD_x\frac{\partial C}{\partial x}\right)\end{pmatrix}, \tilde{F}_2=\begin{pmatrix}0\\0\\0\\\frac{\partial}{\partial y}\left(hD_y\frac{\partial C}{\partial y}\right)\end{pmatrix} \qquad (7)$$

$$S=\begin{pmatrix}0\\-ghS_{fx}-gh\frac{\partial zb}{\partial x}\\-ghS_{fy}-gh\frac{\partial zb}{\partial y}\\0\end{pmatrix}$$

III. NUMERICAL MODEL USED

The flow domain is partitioned into a set of triangular cells or finite volumes, $V_i \subset \mathbb{R}^2$. Let Γ_{ij} be the common edge of two neighbouring cells V_i and V_j, with $|\Gamma_{ij}|$ its length, $N(i)$ is the set of neighbouring triangles of cell V_i, and $\hat{n}_{ij}$ is the unit vector normal to the edge Γ_{ij} and points toward the cell V_j . A cell-centred finite volume method is then formulated where all dependent variables are represented as piecewise constant in the cell as follows:

$$W_i=\frac{1}{|V_i|}\int_{V_i} W\,dV_i \qquad (8)$$

For the triangular elements used here, the integral around the element is written as the sum of the contributions from each edge, such that:

$$\frac{W_i^{n+1}-W_i^n}{\Delta t}|V_i|+\sum_{j\in N(i)}\int_{\Gamma_{ij}}F(W^n,\hat{n})d\Gamma-\sum_{j\in N(i)}\int_{\Gamma_{ij}}\bar{F}(W^n,\hat{n})d\Gamma=\int_{V_i}S(W^n)dV \qquad (9)$$

Where $W_i^n=W(x_i,t_n)$ is the vector of conserved variables evaluated at time level $t_n=n\Delta t$ is the number of time steps, Δt is the time step, and $|V_i|$ is the area of cell V_i . To evaluate the state W_i^n , an approximation is

ISSN: 2319-5967
ISO 9001:2008 Certified
International Journal of Engineering Science and Innovative Technology (IJESIT)
Volume 2, Issue 1, January 2013
required of the convective and diffusive flux terms at each edge of the cell. The integral along the $i-j$ edge of a control volume of the normal flux $F(W^n,\hat{n}) = F_1\hat{n}_x + F_2\hat{n}_y$ can be written:

$$\int_{\Gamma_{ij}} F(W^n,\hat{n})d\Gamma = \Phi(W_i^n, W_j^n, \hat{n}_{ij}).L_{ij} \qquad (10)$$

Where Φ is the numerical flux vector and L_{ij} is the edge length of Γ_{ij}. Herein, the following upwind scheme based on Roe's approximate Riemann solver is employed to determine Φ on the control volume surfaces. At each cell edge [11].

$$\Phi(W_i^n, W_j^n, \hat{n}_{ij}) = \frac{1}{2}\left(F(W_i,\hat{n}_{ij}) + F(W_j,\hat{n}_{ij})\right) - \frac{1}{2}|A(\tilde{W},\hat{n}_{ij}|(W_j - W_i) \qquad (11)$$

In which:

$$|A(\tilde{W}\hat{n}_{ij})| = R(\tilde{W},\hat{n}_{ij})|\Lambda(\tilde{W}\hat{n}_{ij})|L(\tilde{W}\hat{n}_{ij}) \qquad (12)$$

Where, $A(\tilde{W}\hat{n}_{ij})$ is the flux Jacobian evaluated using Roe's average state, R and L are the right and left eigenvector matrices of A, and $|\Lambda|$ is a diagonal matrix of the absolute values of the eigenvector of A. For the system given by Equation (6), the flux Jacobian is given by:

$$A(\tilde{W},\hat{n}_{ij}) = \begin{pmatrix} 0 & n_x & n_y \\ (g\tilde{h} - \tilde{u}^2)n_x - \tilde{u}\tilde{v}n_y & 2\tilde{u}n_x + \tilde{v}n_y & \tilde{u}n_y \\ -\tilde{u}\tilde{v}n_x + (g\tilde{h} - \tilde{v}^2)n_y & \tilde{v}n_x & \tilde{u}n_x + 2\tilde{v}n_y \end{pmatrix} \qquad (13)$$

Which has real and distinct eigenvalues (confirming hyperbolicity) given by:

$$\begin{cases} \lambda_1 = \tilde{u}.n_x + \tilde{v}.n_y + \tilde{c} \\ \lambda_2 = \tilde{u}.n_x + \tilde{v}.n_y \\ \lambda_3 = \tilde{u}.n_x + \tilde{v}.n_y - \tilde{c} \end{cases} \qquad (14)$$

Where $\tilde{c}$ is the wave celerity, and $\tilde{u}, \tilde{v}$ *and* $\tilde{h}$ are Roe average values defined as:

$$\begin{cases} \tilde{h} = \dfrac{h_i + h_j}{2} \\ \tilde{u} = \dfrac{u_i\sqrt{h_i} + u_j\sqrt{h_j}}{\sqrt{h_i} + \sqrt{h_j}} \\ \tilde{v} = \dfrac{v_i\sqrt{h_i} + v_j\sqrt{h_j}}{\sqrt{h_i} + \sqrt{h_j}} \end{cases} \qquad (15)$$

A four point finite volume interpolation is used to evaluate the diffusion flux through an inner edge Γij , so one has:

$$\int_{\Gamma_{ij}} \Delta C.\hat{n}d\Gamma = \int_{\Gamma_{ij}} \frac{\partial C}{\partial n}d\Gamma = \text{meas}(\Gamma_{ij})\frac{C_j - C_i}{d_{ij}} \qquad (16)$$

Where$d_{ij} = d(x_i,\Gamma_{ij}) + d(x_j,\Gamma_{ij})$, and x_i is the intersection of the orthogonal bisectors of the edge Γi and $d(x_i,\Gamma_{ij})$ is the distance between x_i and the edge Γi .

The source terms are balanced by means of a two-dimensional implementation of the upwind scheme proposed by Vazquez et al. [15] for treating the homogeneous part of Saint-Venant equations, and which satisfies the exact conservation C-property. Integration of the source term on the control volume Vi is written:

$$\int_{V_i} S^n(W)dV = \sum_{j\in N(i)} \int_{\Gamma_{ij}} S^n(W,\hat{n}_{ij})d\Gamma \qquad (17)$$

Following Bermudez [5], this approximation is up winded and the source term S^n replaced by a numerical source vectorΨ^n, such that:

ISSN: 2319-5967
ISO 9001:2008 Certified
International Journal of Engineering Science and Innovative Technology (IJESIT)
Volume 2, Issue 1, January 2013

$$\int_{V_i} S^n(W)d\Gamma = \Psi^n(X_i, X_j, W_i, W_j, \hat{n}_{ij})\Gamma_{ij} \qquad (18)$$

At each cell interface Γ_{ij}, the contribution of the source term at the point X_{ij} is defined as the projection of the source term vector in the basis of eigenvectors of the Jacobian matrix. Thus the function source term is:

$$\Psi^n(X_i, X_j, W_i, W_j, \hat{n}_{ij}) = [I - |A(\widetilde{W}, \hat{n}_{ij})|A(\widetilde{W}, \hat{n}_{ij})].\hat{S}^n(X_i, X_j, W_i, W_j, \hat{n}_{ij}) \qquad (19)$$

Where I is the identity matrix, $A(\widetilde{W}, \hat{n}_{ij}$ is the Roe flux Jacobian, and $\hat{S}^n(X_i, X_j, W_i, W_j, \hat{n}_{ij})$ represents an approximation of the source term on the cell interface Γ_{ij}. Its choice is crucia to obtain accurate results. Using states W_i *and* W_j the approximation $\hat{S}^n$ is defined by [5] as:

$$\hat{S}^n(X_i, X_j, W_i, W_j, \hat{n}_{ij}) = \begin{bmatrix} 0 \\ g\sqrt{h_i h_j}\dfrac{H_i - H_j}{d_{ij}} n_{ij}^1 \\ g\sqrt{h_i h_j}\dfrac{H_i - H_j}{d_{ij}} n_{ij}^2 \end{bmatrix} \qquad (20)$$

To obtain higher-order spatial accuracy, the fluxes at each edge are calculated using a piecewise linear function of the state variable **W** inside the control volume. For the cellcentred mesh, the MUSCL (Monotone Upstream Centred Scheme for Conserved Laws) approach is adopted, whereby the left and right values of the states variable are evaluated from:

$$\begin{cases} W_{ij}^L = W_i + \dfrac{1}{2}\nabla W_i.N_{ij} \\ W_{ij}^L = W_j - \dfrac{1}{2}\vec{\nabla} W_j.N_{ij} \end{cases} \qquad (21)$$

In which N_{ij} is the vector distance between the bar centre coordinates of cells V_i and V_j . The normal gradients of the state variables are calculated by minimizing the quadratic function [4]:

$$\theta_i(X,Y) = \sum_{j\epsilon N(i)} |W_i + (x_j - x_i)X + (x_j - x_i)Y - W_j|^2 \qquad (22)$$

The MUSCL approach gives a second-order spatial approximation. However, numerical oscillations can occur when evaluating the normal gradients of the state variables, and so a slope limiter is usually applied. Here we consider two candidate limiters:

(1) The van Albada limiter:

(2) $$g(X,Y) = \begin{cases} 0 & if\ xy < 0 \\ \dfrac{(x^2+\varepsilon)y + (y^2+\varepsilon)x}{x^2+y^2+2\varepsilon} & sinon \end{cases} \quad \text{with } 0 < \varepsilon \le 1 \qquad (23)$$

(3) The minmod limiter, with general form:

$$\begin{vmatrix} \dfrac{\partial^{lim} W_i}{\partial x} = \dfrac{1}{2}\left(\min_{j\epsilon V(i)} sgn\left(\dfrac{\partial W_j}{\partial x}\right) + \max_{j\epsilon V(i)} sgn\left(\dfrac{\partial W_j}{\partial x}\right)\min_{j\epsilon V(i)}\left|\dfrac{\partial W_j}{\partial x}\right|\right) \\ \dfrac{\partial^{lim} W_i}{\partial x} = \dfrac{1}{2}\left(\min_{j\epsilon V(i)} sgn\left(\dfrac{\partial W_j}{\partial x}\right) + \max_{j\epsilon V(i)} sgn\left(\dfrac{\partial W_j}{\partial x}\right)\min_{j\epsilon V(i)}\left|\dfrac{\partial W_j}{\partial x}\right|\right) \end{vmatrix} \qquad (24)$$

For the purpose of time integration, Equation (6) is expressed as:

$$\frac{\partial W}{\partial t} = \varphi(W) \qquad (25)$$

Where ϕ is an operator that includes the transport, diffusion and source terms of the system. For implicit time integration, TVD Runge–Kutta methods [6] or other ODE solvers can be applied to (18) to achieve a suitable order of accuracy in time. For the present work the second-order Runge–Kutta method has been adopted, given by:

$$\begin{aligned} W^{n+1} &= W^n + \frac{\Delta t}{2}\varphi(\overline{W}) \\ \overline{W} &= W^n + \Delta t\varphi(W^n) \end{aligned} \qquad (26)$$

ISSN: 2319-5967
ISO 9001:2008 Certified
International Journal of Engineering Science and Innovative Technology (IJESIT)
Volume 2, Issue 1, January 2013
To ensure stability of the present explicit scheme, the time step is set according to the Courant-Friedrichs Lewy (CFL) criterion [6], giving:

$$\Delta t = CFL \min_{\Gamma_\varphi}\left(\frac{|V_i| + |V_j|}{2|\Gamma_{ij}| max(|(\lambda_1)_{ij}|, |(\lambda_1)_{ij}|)}\right) \quad (27)$$

Where *CFL* is the Courant number (0 < *CFL* <1). For all numerical solutions presented here, the Courant number is set to *CFL* = 0.65.

The boundary conditions are as follows. At a slip wall boundary, the velocity is projected tangentially onto the wall and there is no flux through the solid boundary. At a nonslip wall boundary, $u_n = 0$ and $v_n = 0$. Open boundary conditions are set by the outgoing Riemann invariants for sub-critical inflow and outflow.

IV. TRIANGULAR MESH

To improve computational performance, an optimal mesh is used that is refined in regions of high gradient in the physical variables (e.g. at a flow discontinuity). An adaptive procedure based on multilevel coarsening and refinement is implemented, aimed at constructing an adaptive mesh that dynamically follows the unsteady solution of the physical problem. Initially, a coarse mesh covers the computational domain. From then on, using the solution as it evolves, we establish a criterion function that identifies volumes that should be refined. The adaption criterion is based on the normalized concentration of the pollutant or water level:

$$Crit(\tau_i) = \frac{C(\tau_i)}{\max\limits_{K\in V_i} C(K)} / \frac{h(\tau_i)}{\max\limits_{K\in V_i} h(K)} \quad (28)$$

Where $C(\tau_i)$ and $h(\tau_i)$ are the pollutant concentration and the water depth at cell τ_i. A list (L) is then established of triangles that must either be refined or coarsened based on the value of the adaptation criterion. An array of integers is used to define, for each triangle of the coarse mesh, the level, *m*, of required adaptation. For example, during refinement a hierarchical multi-level of triangles is created (see Figure 1). For more details about the algorithm, we refer the reader to references [8].

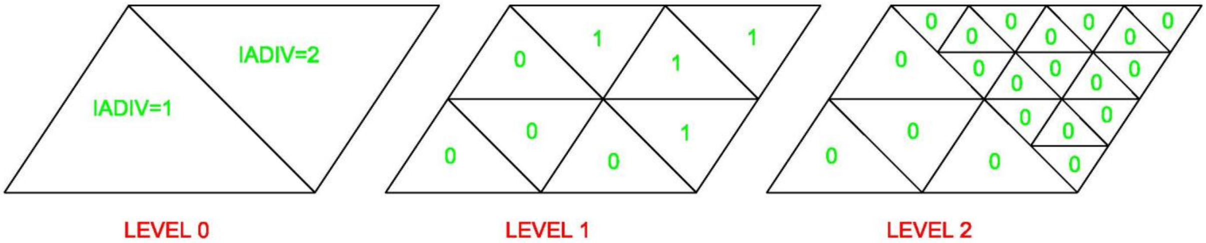

Fig 1: Example of Two Levels of Triangular Mesh Refinement

A. Bathymetry:

Bathymetric slab is necessary to solve nonlinear equations in shallow water; erroneous results are obtained in cases involving a topography (bathymetry) non-uniform. To validate the numerical model to present a serious case of the variation of the field, the model is applied to the problem of reference developed by Goutal [9] of the steady flow over topography. Table 1 shown in Figure 2 shows the bottom topography of the bay to explore.

Table 1: Topography of the Bay of Martil: Projection UTM (Universal Transverse Mercator).

Matricule	X	Y	Z
1	-106024.8771	-1320967.1018	-1.0404
2	-106079.8472	-1320961.4359	-0.8431
3	-106134.8129	-1320955.7706	-0.6458
4	-105639.9566	-1321006.8460	-2.5870
5	-105254.7464	-1321046.8026	-4.5295
6	-104758.5103	-1321099.3359	-9.3527
7	-104543.0917	-1321177.4329	-11.8168

ISSN: 2319-5967
ISO 9001:2008 Certified
International Journal of Engineering Science and Innovative Technology (IJESIT)
Volume 2, Issue 1, January 2013

8	-104598.3582	-1321171.5229	-11.1615
9	-104708.8446	-1321159.7114	-9.8607
10	-104764.0646	-1321153.8116	-9.2175
11	-104929.6378	-1321136.1207	-7.2887
12	-104984.8002	-1321130.2265	-6.6461
n	………………..	………………..	………………..

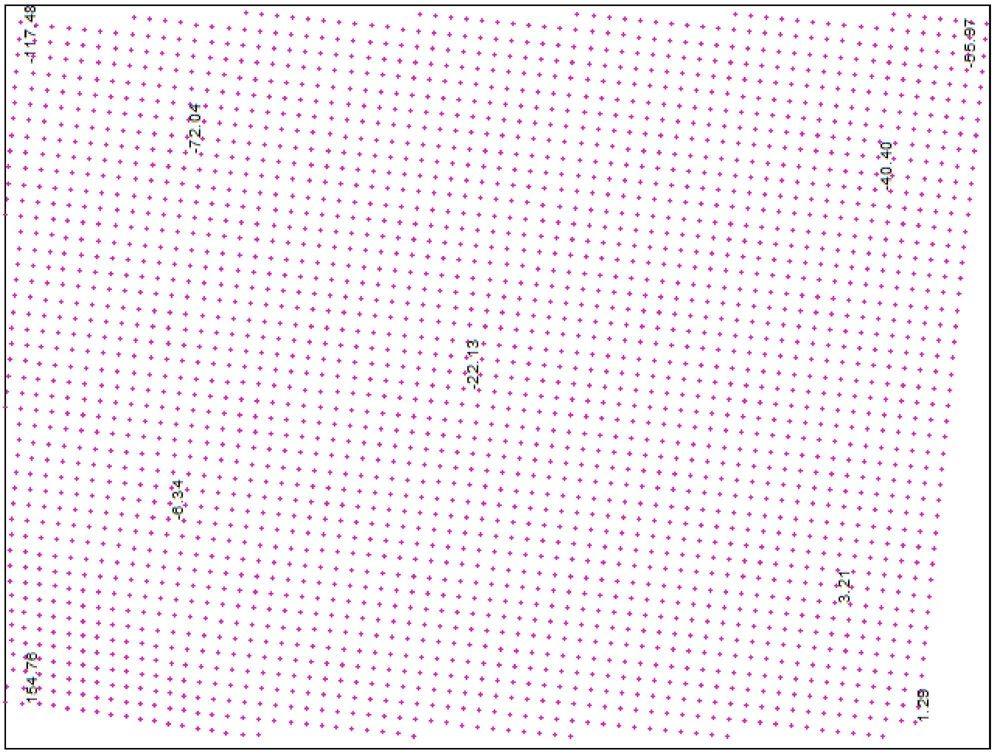

Fig2: Tile bathymetric Bay Martil.

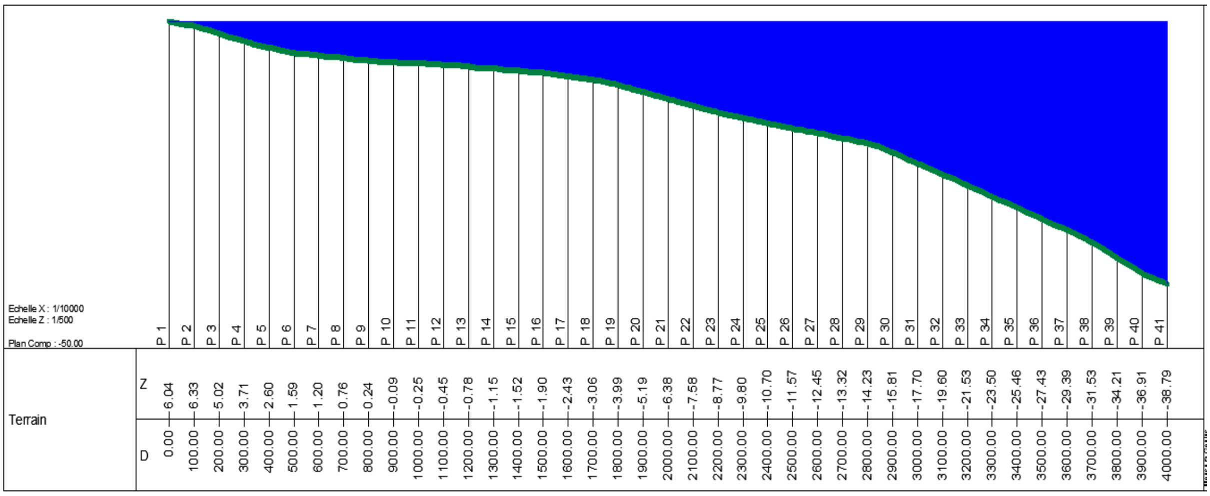

Fig 3: Longitudinal profile of the upper Bay of Martil

ISSN: 2319-5967
ISO 9001:2008 Certified
International Journal of Engineering Science and Innovative Technology (IJESIT)
Volume 2, Issue 1, January 2013

B. Maillage

The two-dimensional laminar flow to a sudden expansion in a side wall is considered as follows, in order to test the ability of the numerical model to reproduce the recirculation zone which develops one behind the step of separating due to flow a step.

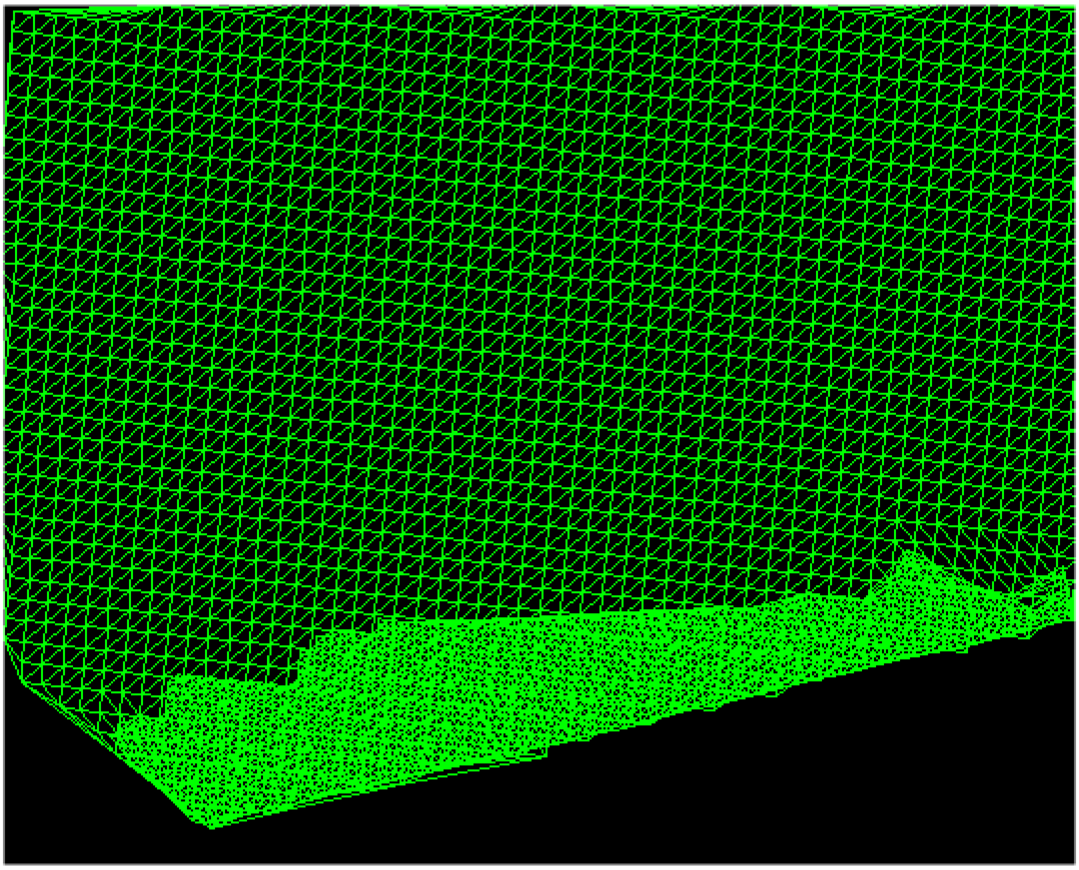

Fig 4: Triangular mesh

V. RESULTS AND DISCUSSION

The simulations presented here test the system for dynamic adaptive an idealized version of the Bay of Martil, noting its complex geometry and nonuniform bathymetry. An initial mesh of 14 536 volumes and 10 253 nodes was created based on the boundary geometry of the Bay of Martil shown in Figure 5. Then the hydrodynamic module was used to simulate the flow field in the bay. At the appointed time, the pollutant was injected into the flow field is fully established. The pollutant concentration injected is given by:

$$C_0 = C_1 exp\left[\frac{(x-x_1)^2+(y-y_1)^2}{r^2}\right] \qquad (29)$$

With the initial concentration is C = 10, x1 = 500m, 4000m and y1 = r = 150m. The diffusion coefficient is constant Dxx = Dyy = 0.001m²/s. Manning's coefficient is $n = 0.001\ s/m^{1/3}$
The flow is forced by a constant velocity profile on the western boundary of the domain, which decreases linearly from 1 m / s at the northwest corner of the field to 0 in the west bank. There is no wetting and drying. Figure 6 shows the results obtained using the van Albada limiter on the adaptive mesh at time t = 2.5, 3.45 h and 6 h. Figure show the distribution of pollutant concentration.

ISSN: 2319-5967
ISO 9001:2008 Certified
International Journal of Engineering Science and Innovative Technology (IJESIT)
Volume 2, Issue 1, January 2013

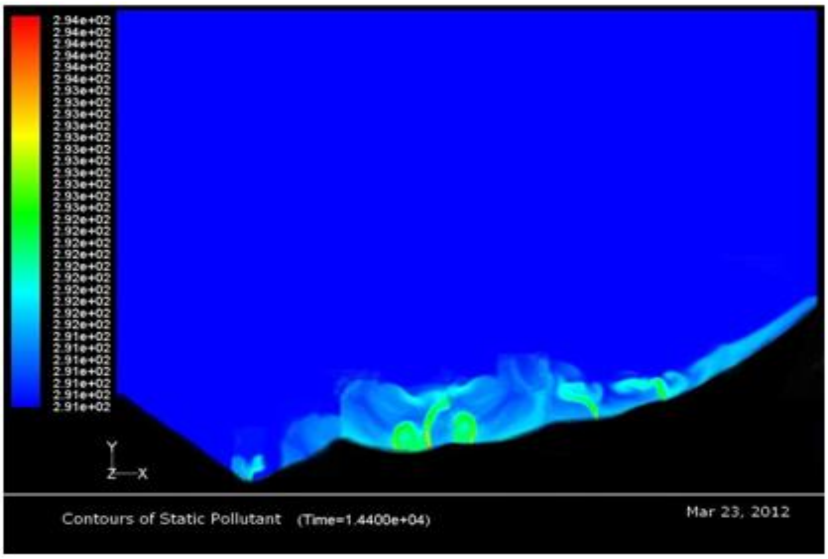

Fig 5: Distribution of pollutant concentration at <u>T=2,5 Hour</u>

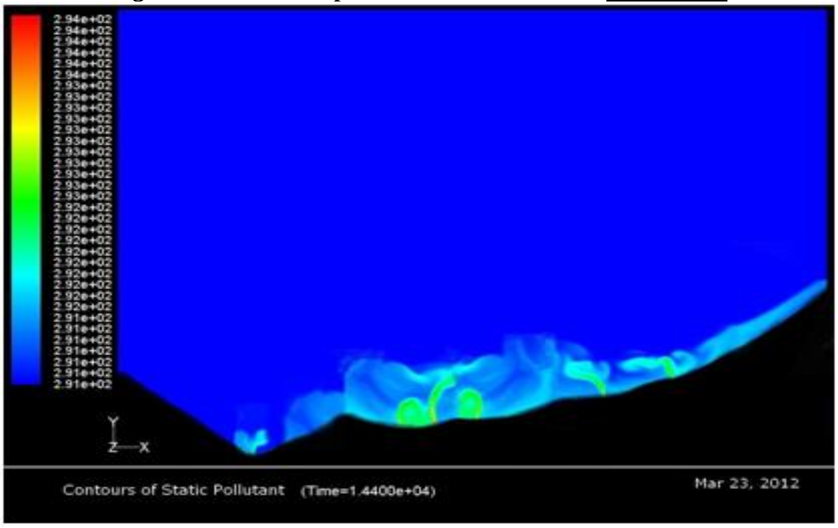

Fig 6: Distribution of pollutant concentration at <u>T=3,45 Hour</u>

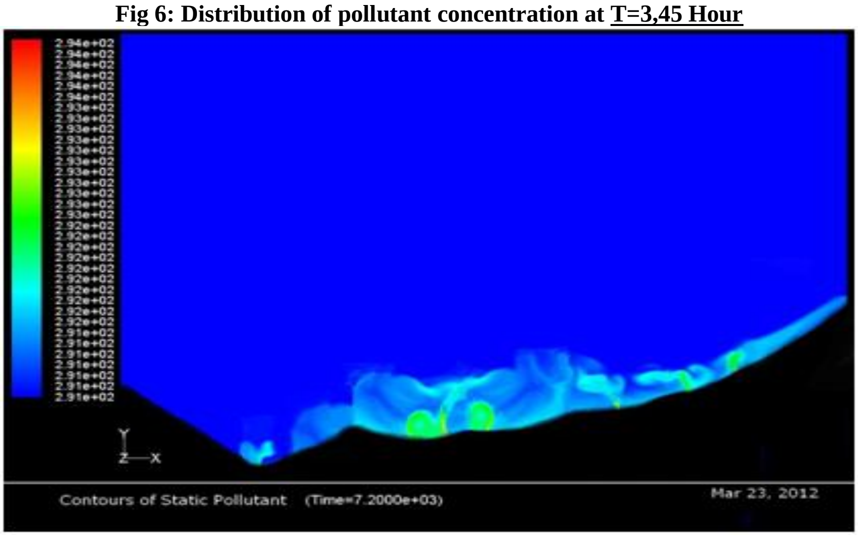

Fig 7: Distribution of pollutant concentration at <u>T=3,45 Hour</u>

ISSN: 2319-5967
ISO 9001:2008 Certified
International Journal of Engineering Science and Innovative Technology (IJESIT)
Volume 2, Issue 1, January 2013

Pollutant concentrations in different mouthpieces are higher because of storm water and wastewater discharges are normally loaded particulate pollutants discharged into the sea through river Martil.

VI. CONCLUSION

This article describes a numerical model to simulate the transport of pollutants in the Bay of Martil. The numerical model solves a couple of nonlinear equation in shallow water and the advection-diffusion equations using a second order Godunov type with the finite volume method on unstructured grids dynamically adaptive.

REFERENCES

[1] Modélisation, Simulation Numerous et Optimization en Génie Côtiers [Damien ISBE].

[2] Theoretical and numerical study of the modeling of unsteady non-isothermal particle-laden turbulent flows by an Eulerian-Eulerian approach [Enrica MASI].

[3] Transport at the Air-Sea Interface, Measurements, Models and Parameterizations [Christoph S. Garbe, Robert A. Handler, Bernd Jhne].

[4] Monthe L., Benkhaldoun F., Elmahi I., "Positivity preserving finite volume Roe schemes for transport diffusion equations", Comp. Meth. In Applied Mech. and Eng. , 178, (1999).

[5] A. Bermudez, A. Dervieux, J.A. Desideri, ME. Vazquez, Upwind schemes for the two-dimensional shallow water equations with variable depth using unstructured meshes, Computer methods in applied mechanics engineering, 155 (1998) 49-72.

[6] Ch. Hirsh. Numerical Computation of internal and external flows: the fundamentals of computational fluid dynamics, volume 1, Wiley & Sons, Second Edition (2007).

[7] Elmiloud Chaabelasri, Contribution à la modélisation des écoulements en eaux peu profondes, avec transport de polluant. (Application à La Baie de Tanger).

[8] N. Goutal and F. Maurel, Procedings of the 2nd workshop on dam-break wave simulation, Laboratoire national d'hydraulique, Groupe Hydraulique Fluviale Electricité de France, France, 1997.

[9] Glaister P. Approximate Riemann solutions of the shallow-water equations. J Hydraul Res 1988; 26(3):293.

[10] Hubbard ME, Garcia-Navarro P. Flux difference splitting and the balancing of source terms and flux gradients. Journal of Computational Physics 2001; 165:89 –125.

[11] Alcrudo F, Garcia-Navarro P. A high resolution Godunov-type scheme in finite volumes for the 2D shallow-water equations. Int J Numer Meth Fluid 1993; 16:489.

[12] Liu X.D., Osher S., Chan T., Weighted essentially non-oscillatory schemes, Journal of Computational Physics 115 (1) (1994) 200–212.

[13] F. Marche, Theoretical and numerical study of shallow water models. Applicationsto near shore hydrodynamics. Ph.D, thesis, Bourdeaux, (2005).

[14] Vazquez-Cendon ME. Improved treatment of source terms in upwind schemes for shallow water equations in channels with irregular geometry. Journal of Computational Physics 1999; 148:497– 526.

[15] Elmahi I., Schémas volumes finis pour la simulation numérique de problèmes à fronts raides [8] en maillages non structurés adaptatifs, Ph.D, thesis, Rouen, 1999.